Catal Lett (2012) 142:205–212
DOI 10.1007/s10562-011-0746-4

Catalytic Steam Reforming of Propane over Ni/LaAlO$_3$ Catalysts: Influence of Preparation Methods and OSC on Activity and Stability

D. Harshini · Chang Won Yoon · Jonghee Han · Sung Pil Yoon · Suk Woo Nam · Tae-Hoon Lim

Received: 9 September 2011 / Accepted: 16 November 2011 / Published online: 6 December 2011

Abstract To develop an efficient catalyst for steam reforming of propane, Ni/LaAlO$_3$ catalysts were prepared by deposition precipitation, impregnation, and solvo-thermal methods, and characterized by XRD, BET, H$_2$-TPR, elemental analyses, and TEM. Ni/Al$_2$O$_3$ and Ni/CeO$_2$ catalysts were also synthesized by the solvo-thermal method for comparison. The Ni/LaAlO$_3$ catalysts exhibited better catalytic performance than both Ni/Al$_2$O$_3$ and Ni/CeO$_2$ catalysts, and activities with Ni/LaAlO$_3$ were found to be dependent upon the preparation methods. In particular, the Ni/LaAlO$_3$ catalyst synthesized by the solvo-thermal method exhibited the highest activity presumably because tetrahydrofuran helps distribute generated Ni nanoparticles onto the catalyst surface in a uniform fashion. In addition, the solvo-thermally prepared Ni/LaAlO$_3$ catalyst was found to be highly stable, with its activity being maintained at least during 100 h. The observed high stability is attributed to the excellent oxygen storage capacity of LaAlO$_3$, which was first determined by thermogravimetric methods as well as by soot oxidations in the presence of Al$_2$O$_3$, CeO$_2$, and LaAlO$_3$. Compared to the Ni/Al$_2$O$_3$ and Ni/CeO$_2$ catalysts, Ni/LaAlO$_3$ exhibited suppressed carbon formation even at lower S/C ratios due to the superior oxygen transport ability of the LaAlO$_3$ support.

Keywords Solvo-thermal method · Steam reforming of propane · Oxygen storage capacity · Ni/LaAlO$_3$ catalysts · Soot oxidation

1 Introduction

Due to the high intrinsic energy efficiencies of fuel cells, hydrogen productions via reforming processes have attracted considerable attentions [1–4]. In general, three types of reforming processes have been employed to obtain hydrogen from a number of fuels including methane, gasoline, and diesel; (i) steam reforming (SR), (ii) partial oxidation, and (iii) autothermal reforming. Owing to its capability to produce high hydrogen contents, the SR method has been widely used in industrial processes. Nickel-based catalysts have known to be highly active for this process, but they have suffered from deactivation by coke formation as well as by sintering of metallic nickel phase under operational conditions [5–9]. The carbon formation can be significantly reduced by replacement of active centers with noble metals, but the cost of the precious metals is still a major drawback for practical use of these catalysts [10–15]. Development of efficient Ni-based heterogeneous catalysts possessing both improved activity and resistance against carbon coking is thus of significant importance to realize economically viable reforming processes.

To enhance activity of a steam reforming catalyst, a number of factors including size of active metal clusters, dispersity of metals on a support, and metal–support interactions should be controlled. Methods of catalyst preparation appear to play an important role in governing these characteristics [16–18]. Reactive Ni-based catalysts have been prepared by sol–gel [18, 19], impregnation [20],

---

D. Harshini · C. W. Yoon (✉) · J. Han ·
S. P. Yoon · S. W. Nam · T.-H. Lim
Fuel Cell Research Center, Korea Institute of Science and Technology, Seoul 136-791, Republic of Korea
e-mail: cwyoon@kist.re.kr

D. Harshini
School of Engineering, University of Science and Technology, Daejon 330-305, Republic of Korea

co-precipitation [17], deposition precipitation [21], and solvo-thermal methods [22, 23]. In particular, Chareonpanich et al. [22] previously reported that Ni catalysts synthesized by a tetrahydrofuran(THF)-mediated solvo-thermal method showed high catalytic activity towards dry reforming reactions of methane. The observed activity resulted from well dispersed Ni active sites onto CeO_2 with small particle size. In addition, utilization of THF as a capping agent, that is usually an organic molecule used to stabilize desired nanoparticles by adsorption, helped prevent aggregation of the in situ generated nickel particles, thus promoting interactions between Ni and CeO_2.

One of the effective approaches to improve stability of a catalyst is to utilize supports that possess high oxygen storage capacities [24, 25]. For example, CeO_2 supported nickel catalysts have shown to possess excellent resistance against carbon coking, with only 2% of carbon being deposited after 24 h in the SR reactions of ethanol [26]. The observed high tolerance of CeO_2 was attributed to oxygen transport capacity coupled with its redox cyclability between reduced and oxidized states of cerium ($Ce^{3+} \leftrightarrow Ce^{4+}$) [27], which promotes chemical transformations from deposited carbons at the surface of a Ni catalyst into gasification products (e.g., CO_2) [28]. Use of pure CeO_2, however, may be discouraged because the ceria support could undergo sintering at high temperatures to decrease its oxygen storage characteristics and catalytic activities [25, 27]. Many efforts have been made to overcome the potential sintering problem of CeO_2 supported Ni catalysts by incorporating nickel in mixed oxide supports (e.g., CeO_2–ZrO_2). Recent studies have suggested that mixed oxides containing ceria with cations such as Zr^{4+}, Al^{3+}, and La^{3+} could enhance catalytic, textural, redox, and oxygen storage properties of ceria, and such mixed oxides also exhibit good thermal stability [29–32]. Alternatively, due to their intrinsic oxygen transport abilities, ABO_3 type perovskite-based supports have been utilized to increase stability of a Ni-containing reforming catalyst. Matsukata and coworkers [33] reported the role of lattice oxygen in both catalytic activities and carbon suppression of methane reforming reactions with Ni supported onto various perovskite oxides prepared by wet-impregnation method. For the steam reforming of methane, authors reported that the nickel particle size (60–80 nm) and the lattice oxygen of the $LaAlO_3$ and $SrTiO_3$ supports played an important role in not only promoting the oxidation of CH_x fragments but also in preventing carbon formation. In addition, Urasaki et al. [34] reported that $LaAlO_3$ support showed high oxygen storage capacity (OSC) to give higher conversions of ethanol. These works drove us to explore nickel catalysts supported onto one of the active perovskites, $LaAlO_3$ for steam reforming of propane.

In the present work, Ni-based catalysts supported onto $LaAlO_3$, CeO_2 and Al_2O_3 were prepared and tested for the SR process of propane. In particular, the Ni/$LaAlO_3$ catalysts were prepared by four different methods and influence of the different syntheses on the catalytic activities was studied. The Ni/$LaAlO_3$ catalyst, specifically prepared by a solvo-thermal method, exhibited high surface area and small nickel particle size, resulting in excellent activities and stabilities for the desired reaction. In addition, OSC of $LaAlO_3$ was proved to be highest among the supports employed in this study, thus effectively suppressing carbon formation on the catalyst. To our best knowledge, it is first reported to employ solvo-thermally prepared Ni/$LaAlO_3$ catalyst for steam reforming of propane and further to measure relative oxygen storage capacity of the $LaAlO_3$ support using thermal gravimetric and soot oxidation methods.

2 Experimental

2.1 Catalyst Preparations

The $LaAlO_3$ powder, used as the catalyst support in this study, was prepared by co-precipitation methods. Aqueous solutions of lanthanum nitrate ($La(NO_3)_3 \cdot 6H_2O$, 65.2 g, 150 mmol) and aluminum nitrate ($Al(NO_3)_3 \cdot 9H_2O$, 56.7 g, 150 mmol) were added slowly into a dilute NH_4OH solution (pH $\sim$ 9) upon vigorous stirring. The formed precipitant was then washed several times with hot water, followed by filtration. The obtained solid was dried at 100 °C overnight, and finally calcined at 800 °C for 2 h in air [35].

Ni/$LaAlO_3$ (10 wt%) catalysts were prepared by four different methods; (1) wet impregnations, (2) deposition precipitations with Na_2CO_3, (3) deposition precipitations with NH_4OH, and (4) solvo-thermal methods. For the wet impregnation, $LaAlO_3$ powder (4.5 g) was impregnated with an aqueous solution (100 mL) of nickel nitrate, $Ni(NO_3)_2 \cdot 6H_2O$ (2.5 g) at room temperature. Following with removal of the excess water by evaporation, the resulting solid was dried at 100 °C overnight and then calcined at 450 °C for 5 h in air. The catalyst obtained by this impregnation method is denoted as Ni-IMP. In a deposition precipitation (DP) method using Na_2CO_3 as a precipitating agent, $LaAlO_3$ powder (4.5 g) was initially suspended in an aqueous solution (100 mL) of $Ni(OAc)_2 \cdot 4H_2O$ (2.12 g). A solution of Na_2CO_3 (0.2 M) was then gradually added until the pH value reached 10, followed by aging for 1 h upon vigorous stirring at 80 °C. The resulting solid was then washed with hot water and dried at 100 °C, followed by subsequent calcination at 450 °C for 5 h in air. The obtained catalyst is designated as Ni-DPS. In a DP method using NH_4OH as a precipitating agent, $LaAlO_3$ powder (4.5 g) was suspended in the aqueous solution of $Ni(NO_3)_2 \cdot 6H_2O$ (2.5 g). A solution of NH_4OH (0.1 M) was then slowly added until the pH value of the mixed solution reached 9 where colorless solids were precipitated. The resulting solution was washed with hot water and filtered. The precipitate was dried at 100 °C and then calcined at 450 °C for 5 h in air. The catalyst obtained by this method is designated as Ni-DPA. For a solvo-thermal method, Ni $(NO_3)_2·6H_2O$ (2.5 g) was dissolved in THF (100 mL) and then added into the $LaAlO_3$ powder (4.5 g). The mixture was agitated at room temperature for 1 h and dried at 100 °C. The dried product was calcined at 450 °C for 5 h in air. The obtained catalyst is designated as Ni-ST. For comparison, 10 wt% of Ni/Al_2O_3 and Ni/CeO_2 were also prepared by the solvo-thermal method.

2.2 Catalyst Characterizations

Powder XRD patterns were obtained with a Rigaku X-ray diffractometer, using CuK_α radiation at 40 kV and 20 mA. Continuous scans were preformed with the scan rate of 0.6°/min in the 2θ ranges of 3–90 °. The Ni particle size on the support was analyzed by Philips-CM30 transmission electron microscope (TEM), operated at 200 kV; catalyst powders were dispersed in isopropyl alcohol, followed by transferring into a holey 400 mesh copper grid. The BET surface areas of the catalysts were analyzed by micrometrics Quantachrome instrument. Elemental analyses for detecting the carbon deposition on the catalysts employed were carried out with a fisions CHNS analyzer (EA 1108). Ni contents were analyzed by inductively coupled plasma (ICP) mass spectroscopy at Korea Institute of Science and Technology. Temperature programmed reduction (TPR) measurements were carried out by using 5% hydrogen in argon ($30\ cm^3$/min, STP), as a reducing gas, in a TPR reactor. The weight (0.05 g) of each sample prepared by different methods was kept constant. Temperature was in a range from 30 to 900 °C, with a heating rate of 10 °C/min. Hydrogen consumptions were monitored by a thermoconductivity detector (TCD).

2.3 Catalytic Activities

The catalytic activities of the as-prepared catalysts were evaluated for the steam reforming of propane. The reactions were carried out in a conventional fixed-bed quartz reactor under atmospheric pressure. In a typical reaction, a desired catalyst (0.3 g) was loaded and pretreated with a stream of 5 vol% H_2/N_2 (30 mL/min) at 700 °C for 2 h prior to the reaction. The catalyst was then flushed with N_2 for 0.5 h and heated to required reaction temperature under N_2. A gaseous mixture of propane, H_2O (vapor) and N_2 (balance) was fed at space velocity (GHSV) of 45,000 h^{-1}. The effluents from the reactor were analyzed by on-line gas chromatography.

2.4 Measurement of Relative Oxygen Storage Capacities for as-Prepared Supports

The potential oxygen storage capacities (OSC) of the supports were evaluated at temperatures ranging from 300 to 900 °C, according to a procedure reported previously [36, 37]. Changes in weight of the sample were monitored by thermogravimetry (TG-DSC analyzer, Q-600) under cyclic heat treatments in flowing nitrogen or dry air. The heating cycle was conducted by heating the sample to 1073 K with consecutive cooling to 150 °C, followed by re-heating to 900 °C. All heating and cooling rates were 5 °C/min. The weight loss of a sample during the second heating cycle was used to determine the degree of the oxygen release properties (δ) [36, 37].

The soot oxidation was carried out by thermo gravimetric analysis (TGA) method in a TG-DSC, Q-600 instrument. The model soot used in this study was carbon black Printex-U which was provided by Degussa. In a typical experiment, a mixture of soot and a desired support with a ratio of 1:4 (1 g:4 g) was milled in an agate mortar for ‘tight contact’ condition before the oxidation reaction. The resulting mixture (13–15 mg) was placed in a TGA crucible and heated up to 1000 °C with a heating rate of 10 °C/min under 100 mL/min of air flow [38, 39].

3 Results and Discussion

3.1 Characterizations of Catalysts

The phase structures of the supports and the reduced catalysts were characterized by XRD, as presented in Fig. 1. For comparison, the XRD peaks of Ni/Al_2O_3 and Ni/CeO_2

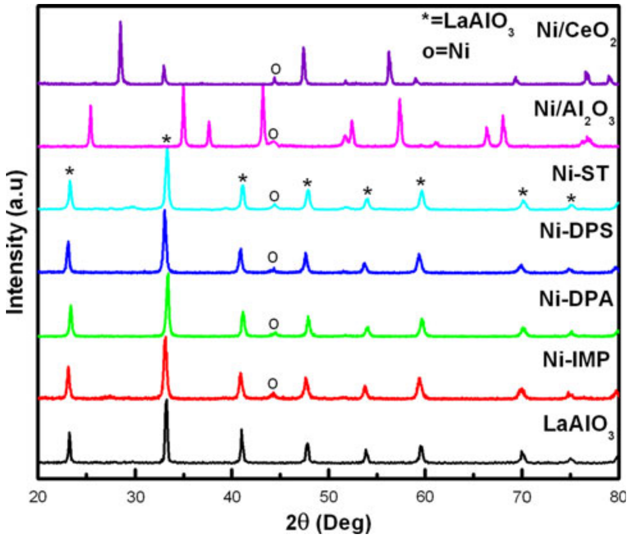

Fig. 1 XRD Spectra of the Ni-based heterogeneous catalysts

Table 1 Calculated surface area and average particle size of the generated Ni nanoparticles

Catalyst	Ni loading by ICP	BET surface area (m^2/g)	Avg. Ni particle size (nm)[a]	Avg. Ni crystallite size (nm)[b]
Ni-IMP	9.49	10	21–23	22.5
Ni-DPA	10.3	14	17–19	18.5
Ni-DPS	10.3	17	14–16	15.3
Ni-ST	10.2	22	8–11	10.6
Ni/Al_2O_3	10.3	26	8–11	10.7
Ni/CeO_2	10.3	19	8–11	10.4

[a] Calculated by TEM

[b] Calculated by XRD

were presented. The $LaAlO_3$ support showed rhombohedral phase in accordance with JCPDS (31-0022). In contrast, all the $Ni/LaAlO_3$ catalysts prepared by four different methods showed metallic Ni phase as well as the rhombohedral $LaAlO_3$ phase, indicating the formation of Ni(0) nano particles onto the $LaAlO_3$ supports. Surface areas, particle sizes, and calculated mean crystallite sizes of the four Ni/$LaAlO_3$ catalysts are listed in Table 1. Compared to those prepared by other methods, the catalyst prepared by solvo-thermal synthesis possessed the highest surface area (22 m^2/g) with lowest particle size (8–11 nm). The observed smaller particle size in the solvo-thermal preparation may be attributed to the utilization of an organic solvent, tetrahydrofuran (THF) which could act as a capping agent and thus prevents aggregation of the formed Ni(0) nano particles [22]. The Ni particles onto Al_2O_3 and CeO_2 supports were observed to be similar in sizes, but surface areas were slightly different (Ni/Al_2O_3 = 26 m^2/g; Ni/CeO_2 = 19 m^2/g).

The H_2–TPR curves of the $Ni/LaAlO_3$ catalysts prepared by various preparation methods are illustrated in Fig. 2. For comparison, the reduction of the $LaAlO_3$ support itself was also carried out under the same conditions. A broad reduction peak at 635 °C was exhibited in the $LaAlO_3$ support but barely seen in the $Ni/LaAlO_3$ catalysts. In the $LaAlO_3$ supported Ni-based catalysts, peaks in the range of 200–400 °C are attributed to the reduction of relatively free NiO particles that contacted with NiO. Peaks at 400–450 °C are responsible for NiO species weakly interacted with $LaAlO_3$, while the reduction peaks observed at >450 °C are attributed to NiO species strongly interacting with the $LaAlO_3$ support [40, 41]. For Ni-DPS, the TPR curve shows a small peak centered at 380 °C, corresponding to the reduction of free NiO dispersed on the $LaAlO_3$ surface. In addition, a broad peak centered at 446 °C with a tail extending to 540 °C was also observed presumably due to the strong interaction of complex NiO with the support. Likewise, the Ni-DPA catalyst exhibited reduction peaks at 408 °C and at 530 °C, respectively. In contrast, the H_2-TPR peaks of the Ni-IMP catalyst showed a relatively sharp peak at 392 °C but no significant signal was observed at >450 °C, indicating the absence of strong interaction between NiO species and the $LaAlO_3$ support in Ni-IMP. In case of the Ni-ST catalyst, a reduction peak centered at 519 °C is significant, again suggesting that the complex NiO species are strongly interacting with $LaAlO_3$. Strong interactions between Ni and $LaAlO_3$ could enhance the mobility of the lattice oxygen atoms in the $LaAlO_3$ support and thus help suppress carbon deposition on the surface of the catalyst during a reforming reaction. Indeed, the Ni-ST catalyst exhibited superior ability against coke formation (vide infra). A reduction peak of Ni/Al_2O_3 at 433 °C is much bigger than that observed at 568 °C. Likewise, Ni/CeO_2 has a major reduction peak at 438 °C with a shoulder centered at ~484 °C. These results imply that relatively small portion of NiO species interacting strongly with either Al_2O_3 or CeO_2 were existed in each catalyst.

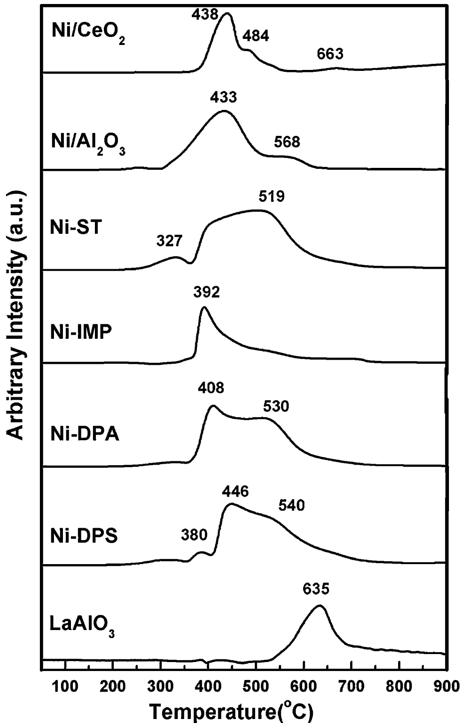

Fig. 2 Temperature-programmed reduction of the Ni-based heterogeneous catalysts

3.2 Catalytic Activities and Stabilities of the Ni/$LaAlO_3$ Catalysts

Catalytic performances towards steam reforming of propane of all $Ni/LaAlO_3$ catalysts were examined at 600–800 °C for 2 h by supplying a mixture of propane, steam, and nitrogen at S/C ratio of 2 and GHSV of

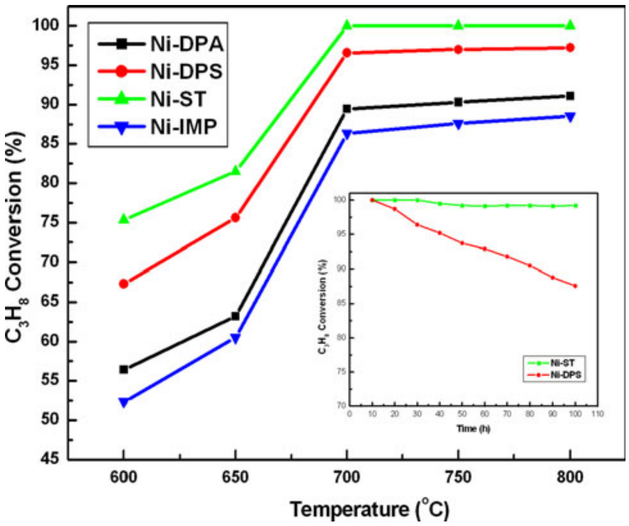

Fig. 3 Profile of propane conversion versus temperature with the Ni/$LaAlO_3$ catalysts: (*Inset*) long-term stability tests with the **Ni-ST** and **Ni-DPS** catalysts

45,000 h^{-1}, respectively. As illustrated in Fig. 3, propane conversions with the Ni/$LaAlO_3$ catalysts prepared by four different methods increased continuously from 600 °C to 700 °C but exhibited little changes in the range of 700–800 °C. The relative catalytic activities are increased in the order of Ni-ST $>$ Ni-DPS $>$ Ni-DPA $>$ Ni-IMP. Note that 100% of propane conversion was achieved with Ni-ST in the range of 700–800 °C. The observed high activity with the Ni-ST catalyst is likely to be attributed to the highest surface area of the catalyst as well as the smallest Ni particle sizes (Table 1). In addition, as supported by H_2-TPR experiments, interactions of the catalytically active Ni(0) species with $LaAlO_3$ could enhance the mobility of the lattice oxygen atoms in the support to prevent deactivation of catalyst via carbon coking. Indeed, the catalytic activity of Ni-ST was maintained at least for 100 h (Fig. 3). Ni-DPS exhibited slightly less activity than Ni-ST but decreased its catalytic performance continuously with time (Fig. 3). The differences in the catalytic performances are likely due to distinctive structures of active sites induced by the preparation methods, and consistent with the previous result [16–18], the solvo-thermal method helped generate well-dispersed, small Ni nano particles on the $LaAlO_3$ support.

Table 2 Propane conversions and amounts of deposited carbon, following reactions with various S/C ratios

Spent catalysts	Propane conversion after 24 h reaction	Amount of carbon deposited (wt%)[a]
Ni-ST (S/C = 2)	100–100	<0.3
Ni-ST (S/C = 1.75)	100–100	<0.3
Ni-ST (S/C = 1.5)	100–96	1.2
Ni-ST (S/C = 1)	100–73	3.3

[a] Obtained from CHN analysis

Stability of the Ni-ST catalyst was investigated by carrying out the steam reforming of propane with various S/C ratios from 1 to 2 for 24 h at 700 °C. Flow rate of propane was kept constant at 50 mL/min with GHSV of 45,000 h^{-1}. Degree of carbon deposition on the catalyst was evaluated by CHN elemental analyses following the reforming reactions. The propane conversions with the S/C ratios of 1.75 and 2.0 were nearly quantitative, whereas the conversions decreased to 96% and 73% with S/C ratios of 1.5 and 1, respectively (Table 2). Consistent with these observed activities, no carbon formations were observed with the S/C ratios of 2 and 1.75 while 1.2 and 3.3 wt% of carbon were deposited on catalyst surface in the case of the S/C ratios of 1.5 and 2, respectively (Table 2). Long-term stabilities of Ni-ST, Ni/Al_2O_3 and Ni/CeO_2 catalysts were also examined at 700 °C for 100 h with the S/C ratio and GHSV of 1.75 and 45,000 h^{-1}, respectively. Contrast to the high stability observed in Ni-ST, the propane conversions of the Ni/Al_2O_3 and Ni/CeO_2 catalysts were drastically decreased with time (Fig. 4). For example, the propane conversions with Ni/Al_2O_3 and Ni/CeO_2 were decreased to 81% and 67%, respectively, after 100 h. In the case of Ni/Al_2O_3 ca. 5.3% of carbon was detected by CHN analysis while no carbon was found in the Ni/CeO_2 catalyst after 100 h. Thus, the as-synthesized Ni-ST catalyst is superior to Ni/Al_2O_3 and Ni/CeO_2 in terms of catalytic activity and stability.

3.3 Influence of OSC on Stability of a Catalyst

To understand the observed catalytic activities, morphologies before and after the long-term stability tests were

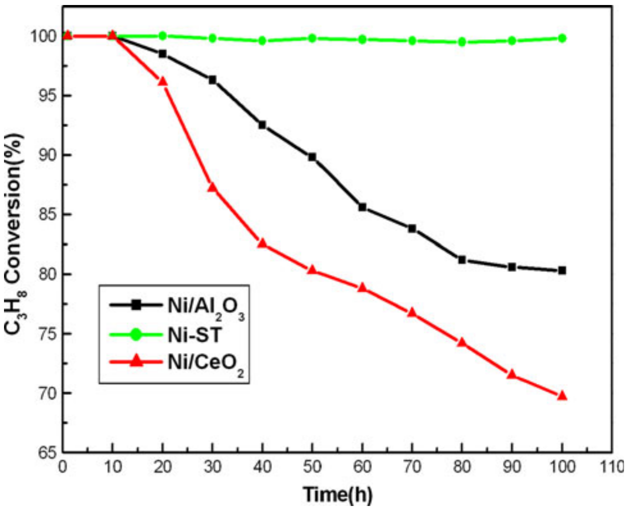

Fig. 4 Long-term stability tests for the steam reforming of propane over **Ni-ST**, Ni/Al_2O_3 and Ni/CeO_2; (**a**) propane conversion and (**b**) H_2 yield versus time

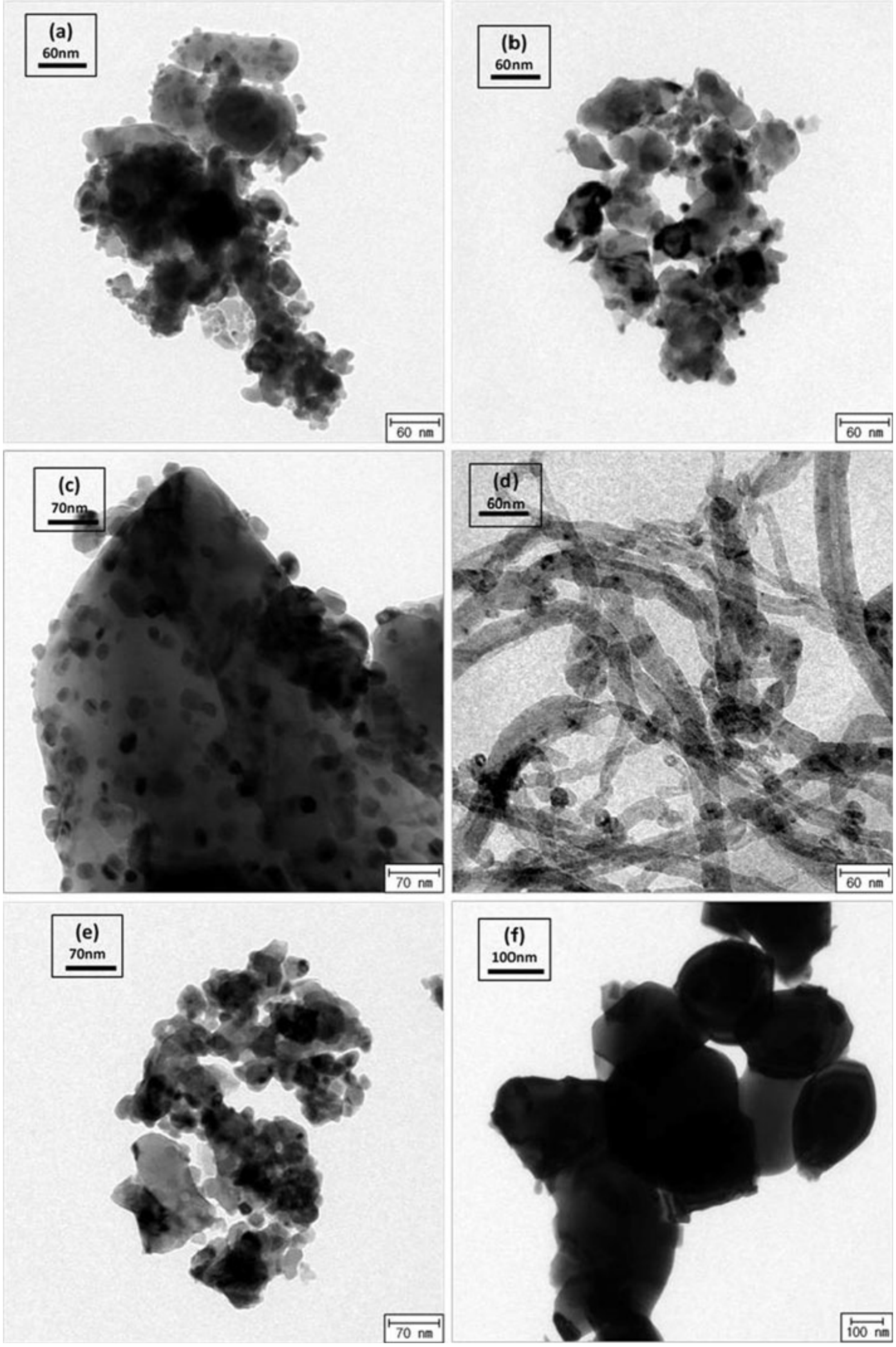

Fig. 5 TEM images of catalysts before and after the reactions: (**a**) **Ni-ST** (before), (**b**) **Ni-ST** (after); (**c**) **Ni/Al$_2$O$_3$** (before), (**d**) **Ni/Al$_2$O$_3$** (after); (**e**) **Ni/CeO$_2$** (before), (**f**) **Ni/CeO$_2$** (after)

characterized by TEM in the Ni-ST, Ni/Al$_2$O$_3$ and Ni/CeO$_2$ catalysts. The size of the active nickel particles onto the Ni-ST catalyst was slightly increased following the steam reforming reaction for 100 h (Fig. 5a, b), with no carbon being found on its surface. In contrast, TEM images of the Ni/Al$_2$O$_3$ catalyst clearly showed the carbon deposition on its surface after 100 h (Fig. 5c, d). In case of the Ni/CeO$_2$ catalyst, the CeO$_2$ supports were sintered significantly, as evidenced by TEM studies (Fig. 5e, f). Following the reforming reaction, the particle size of CeO$_2$ was increased approximately from 70 nm to 200 nm. Consistent with the results obtained by elemental analysis, no carbon was formed on the surface of Ni/CeO$_2$. Therefore, the decreased activity of the Ni/Al$_2$O$_3$ catalyst with time results from catalyst deactivation by carbon coking. For the Ni/CeO$_2$ catalyst, the decreased conversion with time is due to the reduction of surface area, caused by sintering during the reaction [25]. Compared to other catalysts, the Ni-ST catalyst exhibited excellent resistance against coking as well as sintering, leading to the superior performance towards the steam reforming of propane.

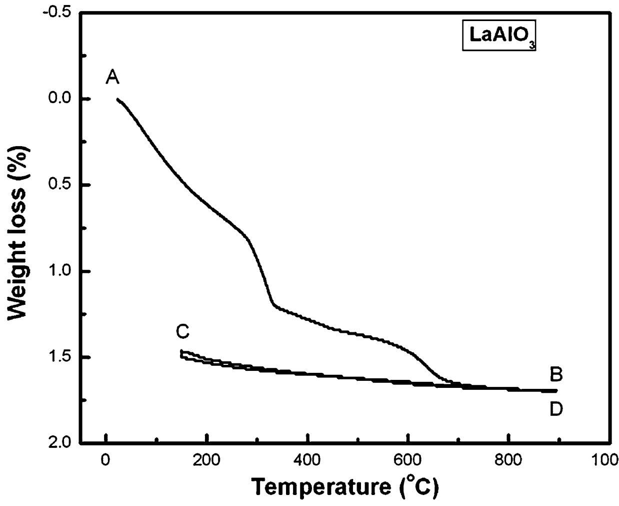

Fig. 6 Sequential thermo-gravimetric analyses to measure oxygen storage capacity of Ni/LaAlO$_3$

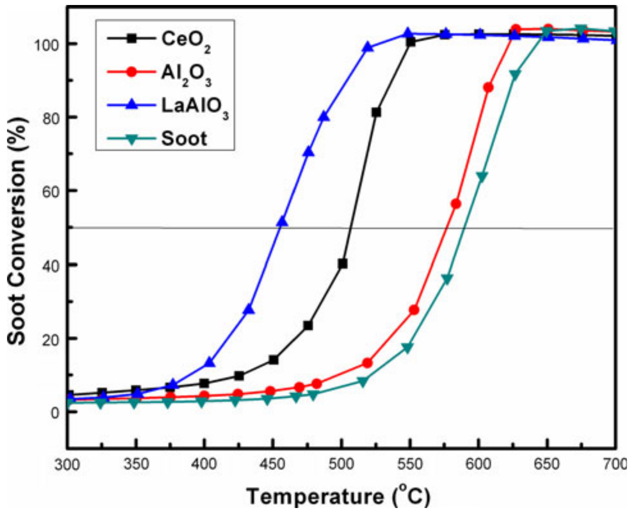

Fig. 7 Soot oxidations in the presence of the CeO$_2$, Al$_2$O$_3$, and LaAlO$_3$ supports

Table 3 Light-off temperatures of the supports observed for the soot oxidations

Catalysts	$T_{1/2}$(°C)
LaAlO$_3$	455
CeO$_2$	508
Al$_2$O$_3$	578
Soot	590

The resistance of CeO$_2$ against carbon formation has been known to be related to the oxygen storage capacity (OSC) of the support [42]; that is, the carbon deposited on the catalyst can further react with oxygen supplied from the CeO$_2$ support to produce gasified products (e.g., CO$_2$). Since the OSC of CeO$_2$ is very high, no carbon was found on the Ni/CeO$_2$ catalyst in this study. Analogously, lattice oxygen atoms in the LaAlO$_3$ support can play pivotal roles in promoting the oxidation of the deposited carbon adsorbed on the Ni/LaAlO$_3$ catalyst. The OSC of a support has previously been measured by thermo gravimetric method (TG). This method was initially applied to the as-synthesized LaAlO$_3$ support (Fig. 6). Firstly, the weight of the support was decreased by 1.7% upon heating the LaAlO$_3$ support from 23 °C to 900 °C, which corresponds to the release of both adsorbed water molecules and oxygen (A → B). Upon consecutive cooling of the support from 900 °C to 180 °C (B → C), the weight was slightly recovered but decreased again by 0.16% in the second heating step (C → D). The observed weight decrease (0.16%) in the second heating stage at the temperature range of 300–900 °C corresponds to the potential oxygen release properties (δ) of 0.05. This value of $\delta = 0.05$ is higher than that ($\delta = 0.04$) of the CeO$_2$ support. The value of δ for Al$_2$O$_3$ was measured to nearly zero, indicating absence of OSC. Consequently, the LaAlO$_3$ support possesses high OSC to suppress the carbon formation on the Ni/LaAlO$_3$ catalyst.

Further evidence to support the high oxygen storage capacity of LaAlO$_3$ was obtained by determining the conversion of soot over the three supports (LaAlO$_3$, Al$_2$O$_3$ and CeO$_2$) as a function of temperature under the flow of air (Fig. 7). Since active oxygen species involved in the soot combustion could come from the gaseous molecular oxygen and/or oxygen ions transported from a support, the oxidation of soot is also tested in the absence of a support to elucidate the effect only from lattice oxygen atoms of a support. Table 3 shows light-off temperature, defined as temperature at 50% conversion ($T_{1/2}$), during oxidation in air for support-soot mixtures prepared in a tight contact method. Al$_2$O$_3$ exhibited a nearly identical conversion profile to the pure soot, as shown in Table 3 and Fig. 7. In contrast, the LaAlO$_3$ and CeO$_2$ supports showed significantly decreased light-off temperatures (455 °C for LaAlO$_3$ and 508 °C for CeO$_2$, respectively) for the soot oxidation. Thus, the enhanced catalytic stability of Ni-ST were attributed to the active lattice oxygen ions generated by oxygen exchange reactions between gas phase O$_2$ and oxygen atoms in the oxide framework along with high resistance against sintering at high temperature.

4 Conclusions

The Ni-based catalysts supported onto LaAlO$_3$, Al$_2$O$_3$, and CeO$_2$ were prepared by various methods and examined their performance in steam reforming of propane. Catalytic activities proved to be remarkably dependent on the preparation methods employed. In particular, the Ni/LaAlO$_3$ catalysts prepared by a solvo-thermal method exhibited the highest activity and stability. High activity was found to be attributed to the relatively well-dispersed, small Ni nano particles on $LaAlO_3$, induced by the solvo-thermal method. The superior stability of Ni/$LaAlO_3$ (Ni-ST) was originated from resistance against sintering at desired high temperature and its high oxygen transport ability, evidenced by both the sequential thermo gravimetric method and the soot oxidations. Thus, the as-synthesized Ni/$LaAlO_3$ catalyst is expected to be used for reforming reactions using various fuels. The identified controlling factors for hydrogen production from propane could provide a valuable insight to develop highly efficient reforming catalytic systems.

Acknowledgments This study was supported financially by the Seoul R&D program. Part of this research was also supported by the Global Research Laboratory Program through the National Research Foundation of Korea funded by the Ministry of Education, Science and Technology of Korea.

References

1. Li Y, Wang X, Xie C, Song C (2009) Appl Catal A 357:213
2. Brown LF (2001) Int J Hydrogen Energy 26:381
3. Song CS (2002) Catal Today 77:17
4. Trimm DL, Onsan ZI (2001) Catal Rev Sci Eng 43:31
5. Ridler DE, Twigg MV (1989) Catalyst handbook, 2nd edn. ICI, Wolf Publishing Ltd., London, p 225
6. Pompeo F, Nichio NN, Souza MMVM, Cesar DV, Ferretti OA, Schmal M (2007) Appl Catal A 316:175
7. Modafferi V, Panzera G, Baglio V, Frusteri F, Antonucci PL (2008) Appl Catal A 334:1
8. Seo JG, Youn MH, Cho KM, Park S, Lee SH, Lee J, Song IK (2008) Korean J Chem Eng 25:41
9. Harshini D, Kwon YC, Han J, Yoon SP, Nam SW, Lim TH (2010) Korean J Chem Eng 27:480
10. Richardson JT, Paripatyadar SA (1990) Appl Catal A 61:293
11. Igarashi, Ohtaka T, Motoki S (1991) Catal Lett 13:189
12. Rostrup-Nielsen JR, Hansen JH (1993) J Catal 144:38
13. Qin DL (1994) J Catal Today 21:551
14. Craciun R, Shereck B, Gorte RJ (1998) Catal Lett 51:149
15. Wang X, Gorte RJ (2001) Catal Lett 73:15
16. Shen J-P, Song C (2002) Catal Today 77:89
17. Seo JG, Youn MH, Jung JC, Song IK (2009) Int J Hydrogen Energy 34:5409
18. Zhang L, Wang X, Tan B, Ozkan US (2009) J Mol Catal A 297:26
19. Blasin-Aube V, Belkouch L, Monceaux J (2003) Appl Catal B 43:175
20. Jo D, Lee JS, Lee KH (2004) J Mol Catal A 222:199
21. Li Y, Zhang B, Tang X, Xu Y, Shen W (2006) Catal Commun 7:380
22. Chareonpanich M, Teabpinyok N, Kaewtaweesub S (2008) In:Proceedings of WCECS,San Francisco, October 22–24
23. Mekasuwandumrong O, Wongwaranon N, Panpranot J, Praserthdam P (2008) Mater Chem Phys 111:431
24. Silva FA, Martinez DS, Ruiz JAC, Mattos LV, Hori CE, Noronha FB (2008) Appl Catal A 335:145
25. Reddy BM, Thrimurthulu G, Lakshmi K (2009) J Phys Chem C 113:15882
26. Adriana M, Katia R, Jacobs G, Uschi M, Burtron H, Lisiane V, Fabio B (2011) Appl Catal B 102:94
27. Reddy BM, Khan A (2003) J Phys Chem B 107:5162
28. Laosiripojana N, Assabumrungrat S (2006) Appl Catal B 66:29–39
29. Sauvion GN, Caillod J, Gourlaouen C (1986) Rhone-Poulenc. Eur.Patent 0207,857
30. Ohata T, Tsuchitani K, Kitayuchi S (1988) Nippon S K, Jpn. Patent 8,890,311
31. Ashley NE, Rieck JS, Grace WR (1991) Co-Conn. U.S. Patent 484,727
32. Cho BK (1991) J Catal 131:74
33. Urasaki K, Sekine Y, Kawabe S, Kikuchi E, Matsukata M (2005) App Catal A 286:23
34. Urasaki K, Tokunaga K, Sekine Y, Matsukata M, Kikuchi E (2008) Catal Commun 9:600
35. Li W, Zhuo MW, Shi JL (2004) Mater Lett 58:365
36. Reddy BM, Khan A, Lakshmanan P (2005) J Phys Chem B 109:3355
37. Ozawa M, Matuda K, Suzuki S (2000) J Alloys Compd 303–304:56
38. Reddy BM, Rao KN (2009) Catal Commun 10:1350
39. Atribak I, Bueno-López A, García-García A (2008) Catal Commun 9:250
40. Wan H, Li X, Ji S, Huang B, Wang K, Li C (2007) J Nat Gas Chem 16:139
41. Roh H, Jun K, Dong W, Chang J, Park S, Joe Y (2002) J Mol Catal A 181:137
42. Sutthisripok W, Sattayanurak S, Sikong L (2008) J Porous Mater 15:519